AAPT PHYSICS EDUCATION | AMERICAN JOURNAL of PHYSICS

Special relativity and the Michelson–Morley interferometer

Reinhard A. Schumacher

Citation: American Journal of Physics **62**, 609 (1994); doi: 10.1119/1.17535
View online: http://dx.doi.org/10.1119/1.17535
View Table of Contents: http://scitation.aip.org/content/aapt/journal/ajp/62/7?ver=pdfcov
Published by the American Association of Physics Teachers

to the relation between rationalized and unrationalized electromagnetic systems," Am. J. Phys. **21**, 281–286 (1953).
[23]Andre J. deBethune and Jerome J. Perez, "Dimensional symmetry of electrical and magnetic quantities in the unrationalized mks system of units," Am. J. Phys. **24**, 584–584 (1956).
[24]E. Katz, "Concerning the number of independent variables of the classical electromagnetic field," Am. J. Phys. **33**, 306–312 (1965).
[25]Bernard Leroy, "Conversion of electromagnetic quantities from mksa to Gaussian units (and vice versa) using dimensional analysis," Am. J. Phys. **52**, 230–233 (1984).
[26]Giovanni Mana, "Electromagnetic quantities and units derived from classical relativistic electrodynamics," Am. J. Phys. **56**, 1081–1085 (1988).
[27]John David Jackson, *Classical Electrodynamics*, 2nd ed. (Wiley, New York, 1975), pp. 191–194.
[28]The assumption we make is not the only possible assumption. An interesting alternative choice is to assign dimensions of magnetic quantities based on the analogy between the electric quantities E, ϵ_0, **P**, and **D** and the magnetic quantities **H**, μ_0, μ_0**M**, and **B**. The analogy we have chosen is more consistent with the modern assumption that **B** rather than **H** is the primary magnetic parameter, while the above analogy is more consistent with the historical assumption that **H** rather than **B** is the primary magnetic parameter.
[29]John David Jackson, *Classical Electrodynamics*, 2nd ed. (Wiley, New York, 1975), p. 819.

Special relativity and the Michelson–Morley interferometer

Reinhard A. Schumacher
Department of Physics, Carnegie Mellon University, Pittsburgh, Pennsylvania 15213

(Received 30 September 1993; accepted 27 January 1994)

We examine the Michelson–Morley interferometer from an inertial frame in which the apparatus is in motion. Our goal is to complete the typical introductory exposition which drops this discussion as soon as the postulates of relativity are introduced. Computing the paths of light in the apparatus depends on understanding the tilting of the half-silvered mirror due to Lorentz contraction, and also the effect of reflecting light from a moving mirror. The traditional ray diagrams of the classical analysis are augmented to show these features more clearly.

I. INTRODUCTION

The Michelson–Morley (MM) experiment is the celebrated experimental result which is usually used to introduce the necessity for a principle of relativity which declares that all inertial reference frames are equivalent, and that the speed of light is isotropic and constant in any inertial frame. Discussions found in most texts leave a few lingering questions which are not answered to our satisfaction. Typically, after presenting the "classical" (ether) analysis of the MM apparatus, and then citing the observed absence of the predicted fringe shift, Einsteinian relativity is postulated and the MM discussion is abruptly dropped. By hypothesis the speed of light is equal in both arms of the interferometer, so the absent fringe shift becomes axiomatic. But with special relativity (SR) in hand, we may revisit the MM apparatus to consider what happens when the experiment is viewed, not from the reference frame in which the interferometer is at rest, but from a frame in which the apparatus is moving with velocity v. In particular, we wish to check the consistency of the nonorthogonal (i.e., oblique) angles of the light rays which arise in such a frame. We also inquire whether the half-silvered mirror at the center of the interferometer correctly reflects the light to and from the interferometer arms, such that light travels in the appropriate "triangular path" in the transverse arm, and correctly brings the longitudinal ray into line with the transverse ray at the detector. We also revisit the purely classical discussion to examine the precise ray angles in that case. These points are not discussed in the standard texts on SR but can be of concern to students who think carefully about the problem.

II. THE TRANSVERSE RAY

Figure 1 shows schematically the path of the transverse ray in the MM interferometer in a reference frame where the apparatus is moving to the right with speed v. The ray, which is vertical in the interferometer rest frame, now makes an angle Θ with respect to the x axis. If we call the length of the arm D, then the time it takes the ray to travel one way between the mirrors is

$$t=\left(\frac{D^2}{c^2-v^2}\right)^{1/2}=\frac{D}{c}\,\gamma, \tag{1}$$

where $\gamma = 1/\sqrt{1-\beta^2}$ and $\beta=v/c$. We can easily compute the angle, Θ, for this geometry as

$$\tan\Theta=D/vt=1/\beta\gamma. \tag{2}$$

We can compare this angle with a result commonly discussed in texts, namely the formula for the aberration of light; this formula is typically obtained either from the Lorentz transformation of a plane wave, or as the high-speed limit of the angle transformation for a moving particle. It is usually discussed in the context of stellar aberration. We have[1],

$$\tan\Theta=\frac{1}{\gamma}\,\frac{\sin\Theta'}{\cos\Theta'+\beta}, \tag{3}$$

where Θ' is the propagation angle with respect to x' in the (primed) interferometer rest frame. For the transverse ray $\Theta'=\pi/2$, so we find $\tan\Theta=1/\beta\gamma$, in agreement with the geometrical approach which led to Eq. (2). This is our first consistency check: the geometry of the triangular light path

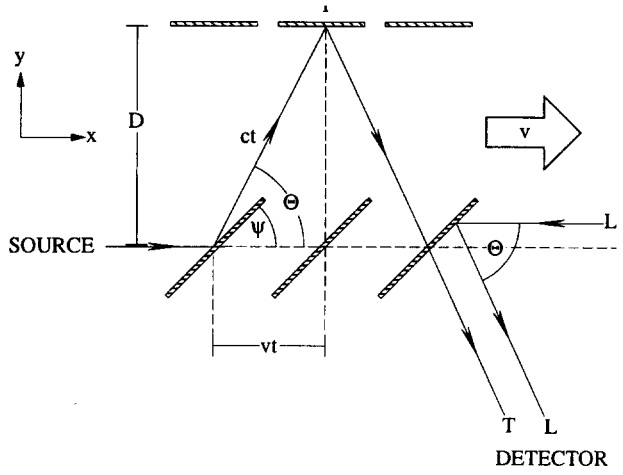

Fig. 1. A Michelson–Morley interferometer moving with velocity v along the x axis. Representative transverse (T) and longitudinal (L) rays are shown. The half-silvered mirror is set at angle ψ; the T ray travels at angle Θ, as does the reflected L ray, if the mirror angle is selected correctly.

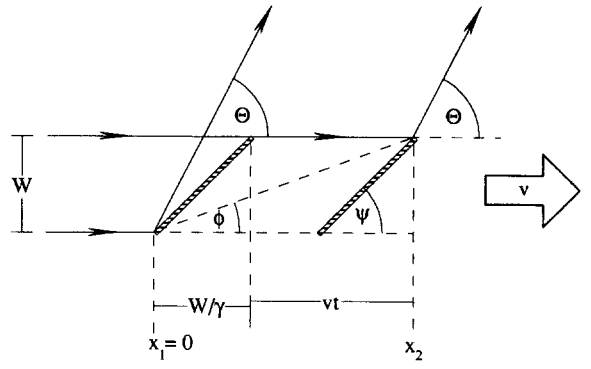

Fig. 2. Rays describing the reflection of a light-front of (arbitrary) width W from a moving mirror (velocity v). Shown are the nominal mirror angle, ψ, the effective mirror angle, ϕ, and the resultant reflection angle Θ. In the SR case, ψ is determined by the Lorentz contraction factor γ.

agrees with the Lorentz transformation for a plane wave of light.

III. THE MOVING MIRROR

The behavior of light reflecting from the moving half-silvered mirror at the center of the apparatus is key to understanding how a ray which was perpendicular to x' in the interferometer rest frame becomes a ray traveling at angle Θ in the new frame where the interferometer is moving. The mirror is adjusted in its rest frame to an angle of exactly $\psi' = 45°$. Measured in the new frame it is Lorentz contracted in the direction of v, making the mirror more perpendicular to the light from the source, and at first glance appears to reflect the light at an angle greater than ninety degrees: the mirror tilts the "wrong" way. In the new frame we have, as seen in Fig. 2,

$$\tan \psi = \gamma, \tag{4}$$

so that ψ is always greater than 45°.

Compensating this tilt of the mirror is the fact that a wave striking a moving surface will reflect at an angle which is velocity dependent. Figure 2 shows the ray optics for the case when the ray coming from the source is reflected into the transverse arm. A wave front of arbitrary width, W, strikes the "bottom" edge of the mirror before the "top" edge, during which time interval, t, the mirror has moved a distance vt. There is therefore an effective angle of the mirror, ϕ, which can be computed using

$$x_2 = ct = \frac{W}{\gamma} + vt,$$

which leads to

$$x_2 = \frac{W}{\gamma}\frac{1}{1-\beta}. \tag{5}$$

From this we have

$$\tan \phi = \frac{W}{x_2} = \gamma(1-\beta) = \sqrt{\frac{1-\beta}{1+\beta}}. \tag{6}$$

The reflected angle, Θ, is twice the effective angle ϕ, just as for the stationary mirror it would be twice ψ. In Eq. (2) we saw that $\tan \Theta = 1/\beta\gamma$. Consistency now demands that

$$\tan \Theta = \tan(2\phi) = 1/\beta\gamma. \tag{7}$$

We proceed using the double-angle identities to obtain

$$\tan \Theta = \frac{2 \tan \phi}{1 - \tan^2 \phi}. \tag{8}$$

With Eq. (6) giving the effective angle of the mirror we obtain

$$\tan \Theta = 2\gamma\frac{1-\beta}{1-\gamma^2(1-\beta)^2} = \frac{1}{\beta\gamma}. \tag{9}$$

This is the desired result. We have verified that light reflecting from the Lorentz-contracted moving mirror is directed at precisely the angle prescribed by the geometry of the moving interferometer, and in agreement with the aberration formula.

We may repeat this type of analysis for the longitudinal arm of the interferometer. Here the question we can ask is whether the returning ray, when it reflects from the Lorentz-contracted mirror, falls into line with the returning transverse ray on the way to the detector. The top edge of the longitudinal wave front now strikes the mirror before the bottom edge, and the mirror has again moved a distance vt in the time interval. The effective angle of the mirror is now steeper than in the previous case, and steeper than 45°. The analog of Eq. (5) now reads

$$x_2 = \frac{W}{\gamma}\frac{1}{1+\beta} \tag{10}$$

and, similar to Eq. (6), we find the effective angle

$$\tan \phi = \frac{W}{x_2} = \gamma(1+\beta) = \sqrt{\frac{1+\beta}{1-\beta}}. \tag{11}$$

The reflected ray satisfies the condition $\Theta = \pi - 2\phi$. The analog of Eq. (8) is

$$\tan\Theta=-\frac{2\tan\phi}{1-\tan^2\phi},$$

which leads to the result, by using Eq. (11),

$$\tan\Theta=-2\gamma\frac{1+\beta}{1-\gamma^2(1+\beta)^2}=\frac{1}{\beta\gamma}. \tag{12}$$

Thus we again find the consistency we seek: The reflected longitudinal ray is parallel to the transmitted transverse ray, and hence the two rays can interfere in the desired way at the detector. The reflection of light from the moving, Lorentz-contracted mirror leads to the correct result.

IV. THE CLASSICAL ANALYSIS

Coming back to the analysis of the interferometer in the classical, pre-SR scenario, we consider the ray and mirror angles. We require the transverse ray still to travel as shown in Fig. 1, interpreting the figure as the classical ether rest frame. The required angle of the ray is seen to be given by $\tan\Theta=1/\beta\gamma$ as before. We also have the relation $\Theta=2\phi$, as before, and so we can solve for the effective angle of the moving mirror as

$$\tan\phi=\gamma(1-\beta). \tag{13}$$

But in the absence of Lorentz contraction of the mirror we have, as the analog to Eq. (6),

$$\tan\phi=\tan\psi_c(1-\beta), \tag{14}$$

where the subscript c is supposed to designate the "classical" case, and so

$$\tan\psi_c=\gamma. \tag{15}$$

Thus in the classical analysis the mirror must, strictly speaking, be tilted at a velocity dependent angle slightly steeper than 45° in order to make the transverse ray follow the correct geometrical path. This effect is second order in v/c, and hence of no detectable consequence in the usual MM setup, as was already clear to Michelson.[2] If we take the mirror to be set "correctly" according to Eq. (15), then the returning longitudinal ray is reflected according to

$$\tan\phi=\tan\psi_c(1+\beta)=\gamma(1+\beta), \tag{14'}$$

in exact algebraic analogy to Eq. (11). The returning longitudinal ray therefore is reflected exactly in line with the transmitted transverse ray, but only if the mirror has been set using *a priori* knowledge of v.

On the other hand, if in the classical analysis the half-silvered mirror is set to exactly 45°, the transverse ray will "overshoot" the desired trajectory while the longitudinal ray will "undershoot." This is illustrated in Fig. 3. Given that $\tan\psi_c=1$, this leads to $\tan\phi=(1\pm\beta)$, for the longitudinal (L) and transverse (T) cases, respectively. Equation (8) then allows us to write, for the ray angles on the way to the detector,

$$\tan\Theta_{L,T}=\frac{1}{\beta}\frac{2(1\pm\beta)}{2\pm\beta}, \tag{16}$$

where the subscripts denote rays from the two arms. In principle, the interference pattern will be dependent on the position of the detector. The difference in these angles is of course exceedingly small; if the difference is called δ, then in the small angle approximation it is easy to show this angle to be

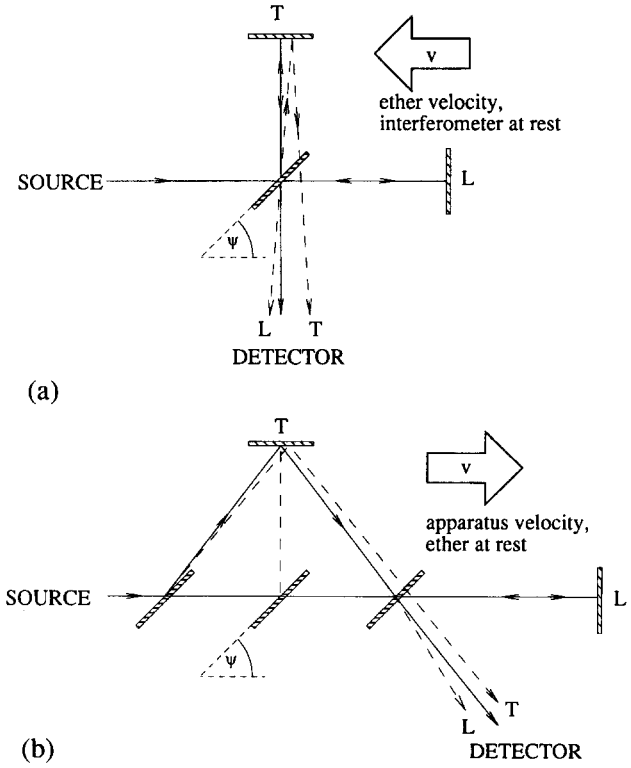

Fig. 3. Classical (no special relativity) diagram of the MM apparatus. Solid lines are for a mirror correctly adjusted such that $\psi=\tan^{-1}\gamma$. Dashed lines for mirror at exactly 45°, showing second order aberration of rays: (a) interferometer rest frame, (b) ether rest frame.

$$\delta=\beta^2\gamma^2, \tag{17}$$

which is of order 10^{-8}, and hence negligible in the usual MM experiment.

V. FURTHER DISCUSSION

We have not discussed the absence of a fringe shift when considering the MM apparatus from the standpoint of SR. This is because the theory gives this basic result by construction, and it is discussed in most texts. The Lorentz-contracted longitudinal arm shortens the travel time in that arm by just the right amount to compensate the smaller travel time, due to the smaller distance covered, in the transverse arm. It is only important to distinguish conceptually between the old Lorentz–Fitzgerald contraction in which the velocity parameter, v, is the interferometer speed with respect to the ether, and the SR Lorentz contraction in which the velocity parameter is the relative speed of the interferometer and the (arbitrary) frame of the observer.

The analysis presented here may be compared with an article by Soni,[3] who also pointed out the importance of considering motion of the mirror in the MM analysis. In that work, however, only first-order results, in v/c, were obtained, and the Lorentz contraction is not taken into account.

VI. SUMMARY AND CONCLUSIONS

We have presented an analysis of the MM interferometer considered from an inertial frame in which the apparatus is

moving with constant velocity. Motivated by a desire to round out the discussion of this famous experiment from the standpoint of special relativity, since standard treatments of the subject omit this point, we see that it provides a useful pedagogical exercise to illustrate some of the well-known features of SR.

In a frame in which the interferometer is moving, the Lorentz contraction of the half-silvered mirror is not the only feature which determines the path of the transverse and longitudinal light rays. The reflection of light from the moving half-silvered mirror, as computed using simple ray optics, must be considered in addition to the Lorentz contraction in order to obtain the correct propagation angles of the light. Having done this, we find consistency between the geometry of the situation and the ray angles computed using the Lorentz transformation via the aberration equation. Reconsidering the classical, pre-special relativity analysis of the MM apparatus, we find that an exact calculation of the angle of the half-silvered mirror results in a velocity-dependent angle which must be set "by hand" if the rays are to follow the correct paths. Ignoring the correction leads to a divergence of the interfering light rays. These effects are of second order in v/c and so are negligible in the MM experiment, but are worth considering to obtain a complete understanding of the physics of the MM interferometer.

[1]Robert Resnick, *Introduction to Special Relativity* (Wiley, New York, 1968).
[2]A. A. Michelson and E. W. Morley, "On the relative motion of the earth and the luminiferous ether," Am. J. Sci. **34**, 333–345 (1887).
[3]V. S. Soni, "A note on the ray diagram of the Michelson–Morley experiment," Am. J. Phys. **56**, 178–179 (1988).

Supersymmetric quantum mechanics: Examples with dirac δ functions

J. Goldstein
Department of Physics, Brooklyn College, Bedford Ave. and Ave. H, City University of New York, New York, New York 11210

C. Lebiedzik and R. W. Robinett
Department of Physics, The Pennsylvania State University, University Park, Pennsylvania 16802

(Received 4 October 1993; accepted 23 December 1993)

We examine the bound-state spectra of several one-dimensional supersymmetric quantum mechanical systems containing Dirac δ-function potentials. Specifically, we investigate the cases of two attractive δ functions, as well as both the infinite well and simple harmonic potentials with an added attractive or repulsive δ function.

I. INTRODUCTION

The study of supersymmetric (SUSY) quantum mechanics, starting with its first elucidation by Witten[1] as a toy example of supersymmetric field theories, has provided new insights into some of the most familiar aspects of nonrelativistic quantum mechanics. (See also the early work of Cooper and Freedman.[2]) Studies of exactly soluble potentials[3,4] and their connection to shape invariance,[5,6] inverse scattering problems,[7] and extensions of the WKB method[5,8] have all used the ideas of supersymmetry to great advantage. The concepts of supersymmetry have even begun to appear in undergraduate textbooks on quantum mechanics (see, e.g., Ref. 9), usually in the context of generalizations of the factorization methods (first introduced by Schrödinger[10] and then extended by Infeld and Hull[11]) often used to elegantly solve the simple harmonic oscillator problem. Since the discussion of this problem using raising and lowering operators is now a standard feature of most such textbooks, the use of supersymmetry to understand the general power of such methods is very appropriate.

Especially at this latter level, because it is often good pedagogy to "learn by doing," it is instructive to have in hand many tractable, analytically soluble examples of one-dimensional supersymmetric quantum mechanical systems for illustrative purposes. Several sets of authors have provided a wide variety of cases for study (see, e.g., Refs. 12–16, and references therein), often based on extensions of simple and rather familiar potentials.

Supersymmetric quantum mechanics, with its fascinating structure of sets of wavefunctions in different potentials giving rise to the same energy spectrum, is also a very natural setting for the use of visualization of wave forms. The ability to make the intuitive connections between the total energy eigenvalue, the potential energy function, and the form of the quantum wave function is a useful goal in a standard undergraduate quantum mechanics course. These connections can be examined in a novel context in SUSY quantum mechanics where the energy eigenvalues are identical, but where the partner potentials are (often dramatically) different. The question of how the partner wave functions "respond" to their corresponding potentials to yield exactly the same energies is an intriguing one. It can often motivate students to examine both the formal structure of the theory in more de-

